Journal Name

ARTICLE

Microcapsules as assay compartments formed through layer-by-layer deposition

Received 00th January 20xx,
Accepted 00th January 20xx

DOI: 10.1039/x0xx00000x

www.rsc.org/

Ali Q. Alorabi, [a,§] Mark D. Tarn, [a, ‡] Martina Stanková, [a] Vesselin N. Paunov, [a] and Nicole Pamme *[a]

We investigate the potential of using microcapsules, generated through layer-by-layer assembly, as reaction compartments for bioassays. A streptavidin-biotin and an esterase-fluorescein diacetate (FDA) assay were employed for proof-of-concept. Streptavidin was incorporated into the microcapsules via two methods: (i) physical adsorption onto $MnCO_3$ microcrystal templates or (ii) co-precipitation with $CaCO_3$ to form mixed microcrystals. The streptavidin-loaded template microparticles were then coated with five bi-layers of polyelectrolytes (polystyrene sulfonate/polyalylamine hydrochloride) $(PAH/PSS)_5$ and the templated cores were dissolved using EDTA to form polyelectrolyte microcapsules loaded with streptavidin. Streptavidin loading of around 77 mg streptavidin per mol of $CaCO_3$ was achieved using the co-precipitation method, compared to 5.1 mg streptavidin per mol of $MnCO_3$ using physical adsorption onto the manganese carbonate crystal surface. The microencapsulated streptavidin was allowed to bind to an analyte which was able to freely diffuse through the polyelectrolyte shell from the aqueous media. Biotin-4-fluorescein was added to the streptavidin-loaded microcapsules, with streptavidin-free capsules serving as the control sample. It was found that both types of microcapsules exhibited a similar fluorescence signal intensity, likely due to non-specific binding of biotin-4-fluorescein to charged groups on the polyelectrolyte shell. Therefore, an alternative esterase-FDA assay was investigated as fluorescence is only produced when FDA penetrates the capsule shell and reacts with the esterase enzyme inside which leads to its hydrolysis. Esterase was loaded into the LbL capsules templated on $CaCO_3$ via co-precipitation. FDA was added to both the esterase-loaded capsules and esterase-free capsules. It was found that the capsules containing esterase fluoresced, while the esterase-free capsules did not. This indicates that the hydrolysis reaction of FDA with esterase occurred inside the LbL microcapsules. These experiments demonstrate the potential of compartmentalised assays to be carried out inside microcapsules which could be applied in complex matrices or in multiplexing experiments, wherein different barcoded microcapsules contain different reagents to provide independent readouts without interference from larger biomolecules present in the surrounding media.

Introduction

Nano- and microcapsules have recently been introduced as drug carrier vesicles. Such capsules are fabricated by a layer-by-layer (LbL) technique involving the deposition of usually up to ten layers of oppositely charged polyelectrolytes (PE) around microparticle templates, such as inorganic microcrystals, colloidal particles (*e.g.* latex) or cells, which are eventually dissolved by an appropriate solvent or reagent leaving a 'hollow' polyelectrolyte capsule.[1] The size of these capsules may range from a few nanometres to hundreds of micrometres depending on the size and the nature of the template employed. [1-3]

LbL capsules are extremely versatile; they may be fabricated using organic templates such as polystyrene[1,4,5] and melamine formaldehyde,[6,7] inorganic templates, *e.g.* SiO_2[4,8] and carbonate particles ($MnCO_3$, $CdCO_3$, $CaCO_3$),[9, 10] or biological cells, *e.g.* red blood cells[11] or yeast cells[12,13] and even droplets.[14,15] These templates can be dissolved by hydrochloric acid (HCl), tetrahydrofuran (THF), hydrogen fluoride (HF), ethylene-diaminetetraacetic acid (EDTA) and sodium hypochlorite (NaClO), respectively. The LbL capsule shell can be fabricated from diverse charged polymers such as poly(ethyleneimine) (PEI), poly(allylamine) (PAH), poly-(diallyldimethylammonium chloride) (PDADMAC) and poly-(styrenesulfonate) (PSS).[16,17] The properties of the LbL capsules can be precisely tailored by appropriate selection of the core template particles and the shell material. LbL capsules have been employed to microencapsulate a wide range of materials ranging from small molecules[18, 19] to macromolecules[20-22] for applications in drug delivery,[23-25] biosensors[26, 27] and bioreactors.[28,29].

Release of molecules from the capsules into the surrounding medium for drug delivery applications has been a particular research focus. More recently, researchers have started to explore the penetration of analytes through the multi-layered wall into the capsules, to use them as miniature reaction

[a] *Department of Chemistry and Biochemistry, University of Hull, Cottingham Road, Hull, HU6 7RX, UK.*
[§] *Current address: Albaha University, Prince Mohammad Bin Saud, Al Bahah 65527, Saudi Arabia.*
[‡] *Current address: School of Earth and Environment, University of Leeds, Woodhouse Lane, Leeds, LS2 9JT, UK.*

Electronic Supplementary Information (ESI) available for characterisation of the PE layers assembled on the microparticles, synthesis of the calcium carbonate microparticles, streptavidin encapsulation efficiencies and the streptavidin-biotin assays. See DOI: 10.1039/x0xx00000x

This journal is © The Royal Society of Chemistry 20xx

Please do not adjust margins

vesicles for analytes of interest to react with biological materials that are encapsulated inside the capsules[21, 30, 31]. For example, Caruso *et al.*[21] reported the encapsulation of catalase enzyme by coating catalase microcrystals with polyelectrolyte layers. The catalase enzymatic activity was preserved and measured by exposing the capsules to hydrogen peroxide in the presence of protease. The polyelectrolyte shell excluded the large protease molecules from the surrounding media, while the hydrogen peroxide diffused through the composite PE shell to interact with the catalase enzyme and produce water and oxygen. In addition, Mak *et al.*[30] developed a method to perform PCR inside polyelectrolyte microcapsules. In this method, the PCR reagents (polymerase, primers and template) were mixed with agarose gel and emulsifier in oil at 40 °C to form microdroplets. The microdroplet emulsion was cooled to form agarose gel microbeads. The microbeads containing the PCR reagents were then coated with multiple PE layers to form a polymeric capsule. During PCR, small molecular weight building blocks, nucleotides (dNTPs), were supplied externally and allowed to diffuse through the permeable capsule wall into the interior, while the resulting high molecular weight PCR products were accumulated within the microcapsule. Moreover, Price *et al.* reported a facile technique for RNA synthesis in LbL microcapsules.[31] Double-stranded DNA (dsDNA) PCR products were adsorbed onto silica colloids followed by LbL assembly of thiol-modified PMA (PMASH) and poly-N-vinylpyrrolidone (PVPON) via hydrogen bonding. After layering, the PMASH was crosslinked and the silica cores were dissolved. Raising the pH disrupted the hydrogen bonding between the PMASH and PVPON, releasing PVPON from the capsules. Diffusion of T7Pol into the capsules initiated transcription from the T7 promoter sequence on the dsDNA template. The synthesized RNA remained entrapped within the capsules.

These examples show the potential of performing reactions inside LbL microcapsules which allow exclusion of larger reactive species from the media. The use of LbL capsules as vessels for bioassays has not yet been fully explored. Conventional immunoassays are carried out in individual reaction tubes or multi-well plates and involve sample pre-purification steps.[32] Miniaturizing immunoassays in LbL microcapsules reduces the sample and reagent volumes. Using microcapsules as assay vessels also opens the door to running many individual or multiplex immunoassays in parallel. The capsule wall can act as a protective barrier to prevent larger molecules entering and interfering with the assay reaction. In the current study, we therefore aimed to investigate the potential of LbL microcapsules to act as reaction vessels for bioassays (figure 1). Streptavidin-biotin and esterase-diacetate fluorescein (FDA) assays were chosen as proof-of-principle bioassays to test this concept.

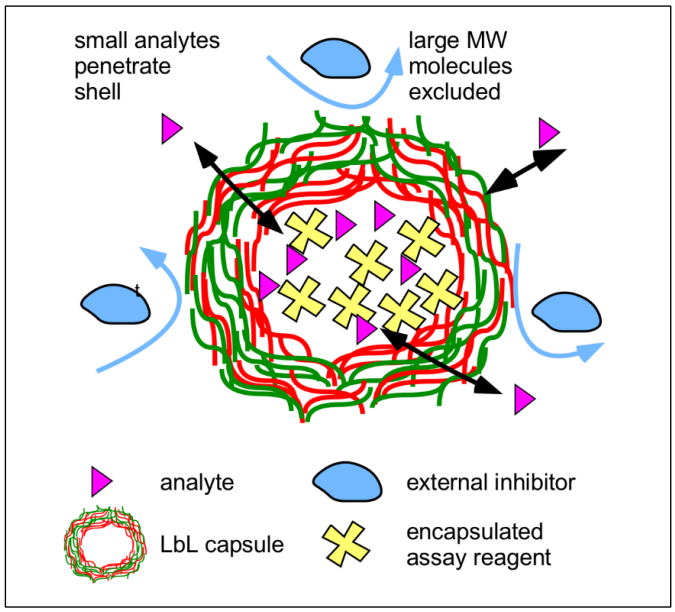

Figure 1. Principle of conducting assays in PE microcapsules prepared by the LbL method using sacrificial templates. The required reagents were encapsulated during the capsule production. Small analyte molecules can penetrate through the capsule shell whilst large molecular weight inhibitors are excluded, allowing extraction of the analyte from the surrounding media for reaction with the encapsulated reagent. This approach is expected to increase the assay selectivity and sensitivity.

Experimental

Materials

Streptavidin, rhodamine red™-X conjugate (λ_{ex} = 570 nm, λ_{em} = 590 nm), unlabelled streptavidin and biotin-4-fluorescein were purchased from Invitrogen Ltd. (UK). Poly(sodium-4-styrenesulfonate) (PSS) (MW 70kDa, powder), poly(allylamine hydrochloride) (PAH) (MW 50kDa, powder), calcium chloride ($CaCl_2$), sodium carbonate (Na_2CO_3), fluorescein diacetate (FDA), esterase from *Saccharomyces cerevisiae* (lyophilized powder) and ethylene-diamine-tetraacetic acid disodium salt dihydrate (EDTA) were all purchased from Sigma-Aldrich (UK) and used as received without further purification.

Preparation of microcapsules from $MnCO_3$ microparticles

$MnCO_3$ microparticles with a size range of 3-5 µm were obtained from PlasmaChem (Germany). The particles were suitable for capsule formation through LbL deposition of PSS and PAH followed by core dissolution as detailed in ESI1. To incorporate streptavidin into the microcapsules, streptavidin was deposited as a first layer in the LbL assembly. 50 mg of the cationic $MnCO_3$ microcrystals were added to 1 mL of fluorescently labelled streptavidin (50 µg mL^{-1}) prepared in phosphate buffered saline (PBS) solution (pH8), to ensure a negative charge on the streptavidin molecules (pI 5.8). The mixture was incubated for 1 h with continuous rotating at 40 rpm on a tube rotator (Keison Products, UK). The streptavidin-coated particles were centrifuged at 5,000 rpm for 3 min, the supernatant was removed and the particles were washed three times with deionised water using centrifugation. Separately,

This journal is © The Royal Society of Chemistry 20xx

Please do not adjust margins

Please do not adjust margins

500 µg mL^{-1} of unlabelled streptavidin was also incubated with $MnCO_3$ using the same protocol for use in the streptavidin-biotin assay.

This was then followed by PE multilayer deposition. Briefly, particles were suspended in 0.5 mL of aqueous NaCl (0.2 M) before adding 1 mL of the cationic PAH polyelectrolyte (2 mg mL^{-1}). The particles were washed three times with deionised water via centrifugation and resuspension, before adding 1 mL of anionic polyelectrolyte (PSS) solution (2 mg mL^{-1}). Five bilayers of (PAH/PSS) were deposited using this procedure. The supernatant and washing solutions were kept for further analysis to determine the encapsulation efficiency from fluorescence measurements. The $MnCO_3$ cores were dissolved with 10 mL EDTA solution (0.3 M) to yield hollow PAH/PSS microcapsules.

Preparation of $CaCO_3$ microspheres

The synthesis of $CaCO_3$ microparticles, the layer-by-layer deposition onto $CaCO_3$ microparticles and core dissolution for capsule formation were performed and optimised as detailed in ESI2. To embed streptavidin in the microcapsules, the protein was co-precipitated with the calcium carbonate. First, 100 µL of fluorescently labelled streptavidin (1 mg mL^{-1}) was added to 900 µL of $CaCl_2$ solution (0.37 M). Then 1 mL of Na_2CO_3 solution (0.33 M) was poured rapidly into this mixture and stirred at 600 rpm for 30 s. With this approach, the streptavidin molecules became intercalated within the precipitated $CaCO_3$ particles. Separately, to form particles for the streptavidin-biotin assay, 500 µL of unlabelled streptavidin (500 µg mL^{-1}) was co-precipitated with 500 µL $CaCl_2$ (0.66 M) and 1 mL of Na_2CO_3 (0.33 M), using the same protocol. Similarly, esterase was co-precipitated into $CaCO_3$ particles by dissolving 10 mg of esterase in 1 mL of $CaCl_2$ (0.33 M) before being rapidly mixed with 1 mL of Na_2CO_3 (0.33 M) and stirred for 30 s. Subsequently, particles were incubated in 1 mL of PAH (1 mg mL^{-1}) under continuous rotation for 15 min. The excess PE was removed by three centrifugation and washing steps with purified water (6,000 rpm, 3 min). Next, the microparticles were dispersed into 1 mL of PSS (1 mg mL^{-1}), followed by three rounds of washing. This LbL deposition was repeated until the desired number of PE layers was deposited on the microparticles. Hollow PE microcapsules were obtained by dissolving the $CaCO_3$ core with EDTA (0.3M).

Assay and enzyme reaction protocols

For the streptavidin-biotin assay, two types of microcapsules with six layers of PAH/PSS were used: (i) microcapsules loaded with streptavidin (non-fluorescently tagged) as well as (ii) microcapsules free of streptavidin as a control. These were incubated with 500 µL (in case capsules templated on $MnCO_3$) or 50 µL (in case capsules templated on $CaCO_3$) of 0.25 mg mL^{-1} of biotin-4-fluorescein for 5 h. The microcapsules were washed with water until the fluorescent biotin was removed. For the esterase-FDA assay, 10 µL of FDA (10 mg mL^{-1} in acetone) was added to esterase-loaded microcapsules and esterase-free microcapsules templated on $CaCO_3$ and then incubated for 10 min.

Streptavidin encapsulation efficiency

To determine the streptavidin encapsulation efficiency in the $MnCO_3$ and $CaCO_3$ particles, fluorescent streptavidin-rhodamine red™-X conjugate was employed. The fluorescently labelled streptavidin was encapsulated as described above. The supernatant containing non-encapsulated streptavidin and all PE and washing solutions were collected. The amount of fluorescent streptavidin in the supernatants were quantified via a fluorescence spectrometer (Perkin Elmer, LS55). The encapsulation efficiency (EE %) was calculated as per equation 1.

$$\text{EE } \% = \frac{(\text{total protein} - \text{free protein in supernatant})}{\text{total protein}} \text{X } 100$$

(equation 1)

Capsule characterization

Confocal Laser Scanning Microscopy (CLSM) images were taken using a Zeiss LSM710 inverted confocal microscope (Zeiss, UK) equipped with 20x, 40x and 63x oil immersion objectives. Samples were prepared by depositing a drop of capsule suspension onto a clean glass slide. The excitation wavelength was 570 nm for the rhodamine-red™-X conjugate, and 490 nm for fluorescein.

Microcapsule suspensions were also observed under a Nikon TE-2000 inverted fluorescence microscope (Nikon, UK), equipped with five objectives (2x, 4x, 10x, 20x, 40x). A high sensitivity black and white digital CCD camera (Retiga-EXL, QImaging, Media Cybernetics, UK) and Image-Pro Plus software (Media Cybernetics, UK) were used to capture images.

Scanning electron microscopy (SEM) was carried out on a Carl Zeiss, EVO 60. The particles and microcapsules were washed with deionised water to remove salts before pipetting onto a glass slide to dry. A thin carbon film was deposited on the particle suspension using a vacuum coating machine (Edwards High Vacuum, E12 series) prior to imaging.

The zeta potential of the coated particle templates was monitored after each PE absorption step during the LbL assembly using a Zetasizer Nano ZS series (Malvern Instruments, UK). Particles were dispersed in Milli-Q water before the measurement. The reported zeta potential is an average of three consecutive measurements.

Please do not adjust margins

Please do not adjust margins

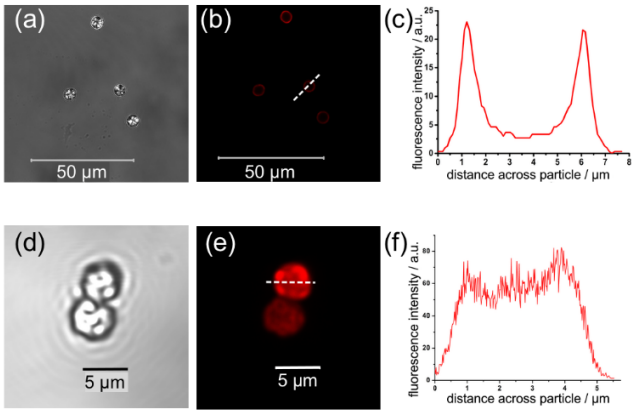

Figure 2 (a) Bright field and (b) confocal microscope images of $MnCO_3$ crystals loaded with rhodamine-X-tagged streptavidin through physical absorption on the particle surface. (c) Fluorescence intensity profile across the $MnCO_3$ particle. (d) Bright field and (e) confocal microscope images of $CaCO_3$ microparticles co-precipitated with fluorescently labelled streptavidin. (f) Fluorescence intensity profile across the $CaCO_3$ particle.

Results and discussion

Encapsulation Efficiency of Proteins

The encapsulation efficiency of rhodamine-streptavidin was determined using two approaches. Firstly, the amount of encapsulated streptavidin was measured directly via fluorescence spectrometry of the particle suspension. Secondly, fluorescence within the PE, washing and EDTA solutions was measured as an indirect method, since some streptavidin could be released during the deposition of PEs and the washing steps, as well as during core dissolution with EDTA.

The encapsulation efficiency of streptavidin on $MnCO_3$ microparticles was investigated by incubating them with fluorescently tagged streptavidin for 1 h. Subsequently, five bilayers of (PAH/PSS) PE were assembled on the particles. Figures 2a and 2b show bright field and fluorescence CLSM images, respectively, for the PE-coated microparticles with encapsulated fluorescent streptavidin. These illustrate the absorption of streptavidin predominately on the external surface of the $MnCO_3$ crystals. The streptavidin did not penetrate inside the core as seen in the CLSM image (fig 2b) and the fluorescence intensity profile through the particle (fig 2c).

We also produced $CaCO_3$ particles loaded with fluorescent streptavidin through co-precipitation from Na_2CO_3 and $CaCl_2$ as described in the experimental section. The streptavidin-loaded $CaCO_3$ particles were washed with Milli-Q water to remove unbound streptavidin before visualisation. The particles were of spherical shape with a fairly narrow size distribution (4 ± 1 µm) (see SEM images, figure S-2.1 in the ESI). Figures 2d and 2e show bright-field and fluorescence microscopy images, respectively, indicating that the streptavidin was embedded successfully. The distribution of the fluorescent streptavidin was observed with CLSM (fig 2e) showing streptavidin throughout the entire volume of the $CaCO_3$ particles. This is further corroborated by the intensity plot (figure 2f) exhibiting a constant fluorescence intensity profile across the particle diameter.

The streptavidin-loaded microparticles ($MnCO_3$ and $CaCO_3$) were coated with five bilayers of (PAH/PSS), followed by dissolution of the core with EDTA (figure 3). There was no noticeable difference in the shape or dimension of microcapsules following the $MnCO_3$ core dissolution. Interestingly, for the $MnCO_3$ templated capsules, the streptavidin was localised in the PE shell rather than being distributed evenly throughout the capsule cavity (fig 3b). The fluorescence intensity profile across the microcapsules showed a high fluorescence intensity at the edge of the microcapsule shell, which decreased as it approached the capsule's centre (figure 3c). A similar effect was seen for the $CaCO_3$-based capsules (fig 3 d-f). This indicates that the streptavidin is likely to be attached to the PE shell.

For $MnCO_3$, it was found that 5.3% of total utilised streptavidin (50 µg) adhered to the microparticles, which was reduced to 4.4% during the PE deposition and washing steps (see ESI 3.1, figure S3.1 and S3.2). Once the PE layers were deposited, it was found that only a negligible amount of streptavidin escaped during core dissolution with EDTA indicating the feasibility of retaining larger molecular weight compounds inside the capsule. The trapping efficiency can be estimated at 51 mg streptavidin per mol of $MnCO_3$. For the $CaCO_3$ particles, it was found that 94% of the utilised streptavidin (100 µg) was entrapped inside the co-precipitated crystals (see ESI 3.2, figures S3-3 and S3-4). During the LbL deposition with PE and washing steps, this was further reduced to 51%. Once again, the particle template dissolution via EDTA solution did not lead to further streptavidin losses (see figure S-2.2, in ESI). The trapping efficiency can be estimated at 77 mg streptavidin per mol of $CaCO_3$.

LbL microcapsules for streptavidin-biotin assay

The streptavidin-biotin assay experiments were conducted with capsules templated on $MnCO_3$ and $CaCO_3$ particles. Two types of microcapsules were fabricated: (i) microcapsules not containing any streptavidin as control, and, (ii) microcapsules with (non-fluorescent) streptavidin. Both kinds of microcapsules were incubated with biotin-4-fluorescein according to the procedure outlined in the experimental section.

This journal is © The Royal Society of Chemistry 20xx

Please do not adjust margins

Please do not adjust margins

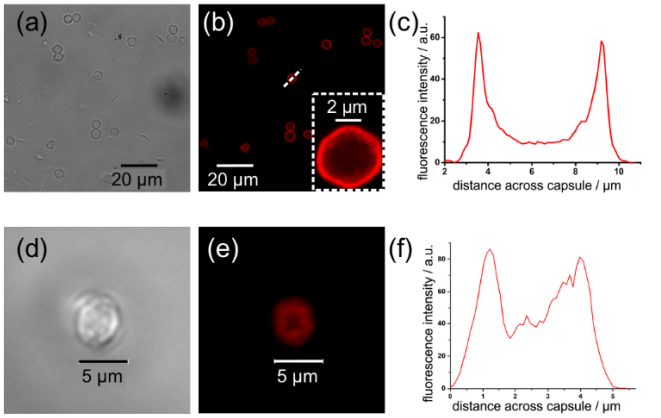

Figure 3 (a) Bright field and (b) confocal microscope images of LbL-coated $MnCO_3$ microparticles following dissolution of the particle core with EDTA. The particles had been prepared by physically adsorbing rhodamine-X-labelled streptavidin onto the particles surface. (c) Fluorescence intensity profile across the $MnCO_3$ particle. (d) Bright field and (e) confocal microscope images of LbL-coated $CaCO_3$ microparticles, following dissolution of the core with EDTA. The core particles had been prepared via co-precipitation of $CaCO_3$ with fluorescently tagged streptavidin. (f) Fluorescence intensity profile across an individual $CaCO_3$ microcapsule.

It was found that both microcapsules containing streptavidin as well as microcapsules entirely free of streptavidin exhibited a fluorescence signal, indicating binding of fluorescently-tagged biotin to the PE capsules regardless of whether streptavidin was present or absent. The fluorescence was localised on the capsule shells, compared to the interior of the capsules, as illustrated by the fluorescence intensity profile plotted across the centre of the PE capsules (see ESI4). This would indicate that the biotin-4-fluorescein adsorbed onto the capsule PE shell rather than freely penetrating into the capsule interior to bind to streptavidin specifically. The negatively charged fluorescein-tagged biotin, upon binding to the cationic polyelectrolyte component of the PE shell, would prevent the biotin molecules from entering and interacting with the streptavidin inside the capsule. To overcome this issue, we designed a different experiment with a non-ionisable molecule (fluorescein diacetate) which is hydrolysed by an esterase enzyme inside the microcapsules upon hydrolysis.

LbL microcapsules for esterase-fluorescein diacetate (FDA) reaction

The esterase enzyme was encapsulated in $CaCO_3$ particles via co-precipitation as outlined in the experimental section. The esterase-loaded $CaCO_3$ particles were then coated with alternating anionic and cationic PE layers and, after the desired number of PEs layers were deposited, the cores were dissolved with EDTA to form hollow PE microcapsules with entrapped esterase. As a control, PE microcapsules free of esterase were also fabricated using the same protocol. Both types of PE microcapsules, esterase-free and esterase-loaded, were incubated with a FDA solution. As can be seen in figure 4a-b, the esterase-free microcapsule exhibited no fluorescence after adding the FDA solution, whereas the esterase-containing capsules showed a fluorescence signal (figure 4c-d). The non-fluorescent FDA molecules, after diffusion into the microcapsule, were hydrolysed by the esterase enzyme to form a fluorescent product, fluorescein. This product was not formed in the capsules free of esterase enzyme. The enzyme-filled microcapsules were imaged with a confocal fluorescence microscope (figure 4e-f). The intensity plot across a capsule (figure 4g) indicates fluorescence on/inside the shell as well as to some degree inside the capsule. The hydrolysis of FDA to fluorescein was successfully demonstrated in the microcapsules. However, it was difficult to determine enzyme localisation in the capsules. The enzyme may have been located in the capsule's centre where the FDA converted to a negatively charged fluorescein. In such a case, the fluorescein would have bound to the cationic PEs on the capsule's internal shell. Another, more realistic possibility is that the esterase enzyme is attached to the inner PE shell, just as was found with the streptavidin, and the incoming FDA is hydrolysed there, where the produced fluorescein also gets deposited.

The observed result was in agreement with studies by other authors using PE microcapsules to immobilise enzymes inside a microcapsule cavity or within PE shells.[21, 28, 33, 34] We have here shown the ability of the system to perform an assay and an enzyme reaction which can be adapted for drug concentration determination by immobilising antibody (protein) in the PE capsules, whilst allowing small analyte molecules (drug) in the sample to penetrate the PE shell to interact with the immobilized protein. Such microcapsule assays could be used for conducting a large number of individual assays in parallel on a small volume of sample for multiplexing.

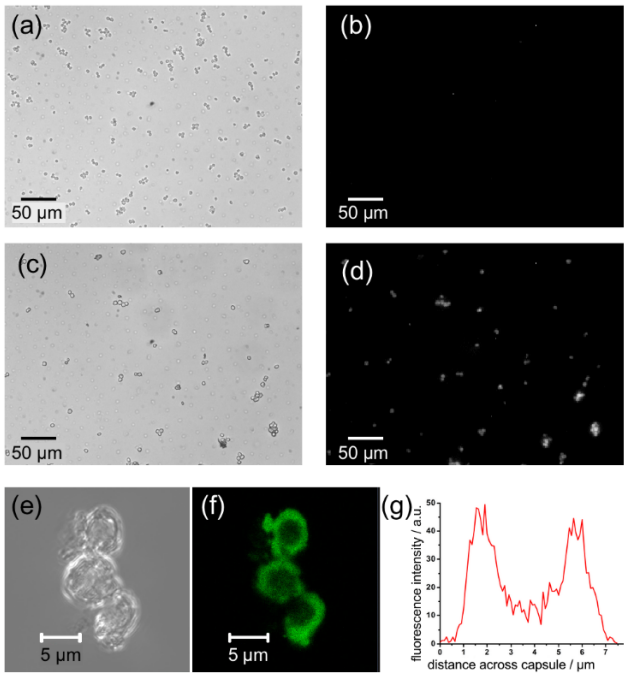

Figure 4 (a) Bright field and (b) fluorescence microscopy images of esterase-free microcapsules following the reaction with FDA. (c) Bright field and (d) fluorescence microscopy images of esterase-loaded microcapsules following the reaction with FDA, showing the formation of the fluorescent product (fluorescein) in the PE capsule. (e) Bright field and (f) fluorescence CLSM images of the esterase-loaded microcapsules following reaction with FDA. (g) Fluorescence intensity profile across an individual microcapsule following the reaction between the FDA and the encapsulated esterase.

This journal is © The Royal Society of Chemistry 20xx

Please do not adjust margins

Please do not adjust margins

Conclusions

The encapsulation of streptavidin and esterase into PE microcapsules fabricated from multiple bilayers of PAH/PSS onto inorganic crystal templates was demonstrated. A biotin-streptavidin assay and an FDA-esterase specific reaction were investigated with these capsules. The biotin-streptavidin assay revealed that biotin was found to bind non-specifically to the PE shell surface and did not penetrate freely into the capsule. For the FDA-esterase reaction, the non-fluorescent starting molecule FDA was used as an analyte model and added to both esterase-filled and esterase-free microcapsules. When the FDA diffused through the microcapsule shell, the esterase enzyme hydrolysed the incoming FDA to fluorescein. This fluorescent product was only observed in the esterase-loaded capsules. This proof-of-concept experiment shows the potential for performing assays for example for drug testing by immobilising specific antibodies inside the PE microcapsule while small sample analytes are allowed to penetrate the capsule shell. Our findings tie in with previous literature reports on enzymatic reactions carried out inside such capsules namely catalase for reaction with penetrating hydrogen peroxide[21] and PCR with penetrating nucleotide building blocks.[30] Microcapsules could react as containers for challenging matrices that may contain inhibiting substances such as environmental soil and water samples and biological samples including stool and urine samples. The method only requires a small volume of sample, the binding reaction is protecting from inhibiting larger size molecules that may be present in the sample and cannot penetrate the capsule shell. Using different coloured or fluorescently-tagged labels, the capsules have the potential to allow parallel analysis of several analytes for multiplex assays.

Conflicts of interest

There are no conflicts to declare.

Acknowledgements

The authors would like to thank the Royal Embassy of Saudi Arabia Cultural Bureau in London and Al-Baha University in Saudi Arabia for funding support. Dr Cordula Kemp and Dr Tony Sinclair are acknowledged for obtaining the CLSM and SEM images, respectively.

Supplementary data

Supplementary data related to this article can be found in the ESI.

References

1. F. Caruso, R. A. Caruso and H. Möhwald, *Science*, 1998, **282**, 1111-1114.
2. E. Donath, G. B. Sukhorukov, F. Caruso, S. A. Davis and H. Mohwald, *Angew. Chem. Int. Edit.*, 1998, **37**, 2202-2205.
3. G. B. Sukhorukov, E. Donath, S. Davis, H. Lichtenfeld, F. Caruso, V. I. Popov and H. Möhwald, *Polym. Advan. Technol.*, 1998, **9**, 759-767.
4. B. V. Parakhonskiy, M. F. Bedard, T. V. Bukreeva, G. B. Sukhorukov, H. Mohwald and A. G. Skirtach, *J. Phys. Chem. A*, 2010, **114**, 1996-2002.
5. C. Déjugnat, D. Haložan and G. B. Sukhorukov, *Macromol. Rapid Commun.*, 2005, **26**, 961-967.
6. G. B. Sukhorukov, E. Donath, H. Lichtenfeld, E. Knippel, M. Knippel, A. Budde and H. Mohwald, *Colloid Surface A*, 1998, **137**, 253-266.
7. A. J. Khopade and F. Caruso, *Chem. Mater.*, 2004, **16**, 2107-2112.
8. S. Sivakumar, V. Bansal, C. Cortez, S. F. Chong, A. N. Zelikin and F. Caruso, *Adv. Mater.*, 2009, **21**, 1820-+.
9. G. B. Sukhorukov, D. V. Volodkin, A. M. Günther, A. I. Petrov, D. B. Shenoy and H. Möhwald, *Journal of Materials Chemistry*, 2004, **14**, 2073-2081.
10. A. A. Antipov, D. Shchukin, Y. Fedutik, A. I. Petrov, G. B. Sukhorukov and H. Möhwald, *Colloids and Surfaces A: Physicochemical and Engineering Aspects*, 2003, **224**, 175-183.
11. B. Neu, A. Voigt, R. Mitlöhner, S. Leporatti, C. Gao, E. Donath, H. Kiesewetter, H. Möhwald, H. Meiselman and H. Bäumler, *Journal of microencapsulation*, 2001, **18**, 385-395.
12. M. L. Brandy, O. J. Cayre, R. F. Fakhrullin, O. D. Velev and V. N. Paunov, *Soft Matter*, 2010, **6**, 3494-3498.
13. R. F. Fakhrullin, J. Garcia-Alonso and V. N. Paunov, *Soft Matter*, 2010, **6**, 391-397.
14. C. Kantak, S. Beyer, L. Yobas, T. Bansal and D. Trau, *Lab Chip*, 2011, **11**, 1030-1035.
15. A. Q. Alorabi, M. D. Tarn, J. Gomez-Pastora, E. Bringas, I. Ortiz, V. N. Paunov and N. Pamme, *Lab Chip*, 2017, **17**, 3785-3795.
16. G. B. Sukhorukov, E. Donath, H. Lichtenfeld, E. Knippel, M. Knippel, A. Budde and H. Möhwald, *Colloids and Surfaces A: physicochemical and engineering aspects*, 1998, **137**, 253-266.
17. C. S. Peyratout and L. Daehne, *Angewandte Chemie International Edition*, 2004, **43**, 3762-3783.
18. W. Song, Q. He, H. Möhwald, Y. Yang and J. Li, *Journal of Controlled Release*, 2009, **139**, 160-166.
19. F. Caruso, W. Yang, D. Trau and R. Renneberg, *Langmuir*, 2000, **16**, 8932-8936.
20. R. Georgieva, S. Moya, M. Hin, R. Mitlöhner, E. Donath, H. Kiesewetter, H. Möhwald and H. Bäumler, *Biomacromolecules*, 2002, **3**, 517-524.
21. F. Caruso, D. Trau, H. Möhwald and R. Renneberg, *Langmuir*, 2000, **16**, 1485-1488.
22. A. Yu, Y. Wang, E. Barlow and F. Caruso, *Advanced Materials*, 2005, **17**, 1737-1741.
23. M. M. de Villiers and Y. M. Lvov, *Journal*, 2011.
24. S. De Koker, R. Hoogenboom and B. G. De Geest, *Chemical Society Reviews*, 2012, **41**, 2867-2884.
25. W. Tong, X. Song and C. Gao, *Chemical Society Reviews*, 2012, **41**, 6103-6124.
26. M. McShane and D. Ritter, *J. Mater. Chem.*, 2010, **20**, 8189-8193.
27. P. Rivera_Gil, M. Nazarenus, S. Ashraf and W. J. Parak, *Small*, 2012, **8**, 943-948.

 This journal is © The Royal Society of Chemistry 20xx

Please do not adjust margins

Please do not adjust margins

28. E. W. Stein, D. V. Volodkin, M. J. McShane and G. B. Sukhorukov, *Biomacromolecules*, 2006, **7**, 710-719.
29. W. Qi, L. Duan and J. Li, *Soft Matter*, 2011, **7**, 1571-1576.
30. W. C. Mak, K. Y. Cheung and D. Trau, *Adv. Funct. Mater.*, 2008, **18**, 2930-2937.
31. A. D. Price, A. N. Zelikin, K. L. Wark and F. Caruso, *Adv. Mater.*, 2010, **22**, 720-723.
32. S. X. Leng, J. E. McElhaney, J. D. Walston, D. X. Xie, N. S. Fedarko and G. A. Kuchel, *J. Gerontol. A-Biol.*, 2008, **63**, 879-884.
33. P. Pescador, I. Katakis, J. L. Toca-Herrera and E. Donath, *Langmuir*, 2008, **24**, 14108-14114.
34. N. G. Balabushevich, G. B. Sukhorukov and N. I. Larionova, *Macromol. Rapid Commun.*, 2005, **26**, 1168-1172.

This journal is © The Royal Society of Chemistry 20xx

Please do not adjust margins

Electronic Supplementary Information (ESI)

Microcapsules as assay compartments formed through layer-by-layer deposition

Ali Q. Alorabi, [a,§] Mark D. Tarn, [a, ‡] Martina Stanková, [a] Vesselin N. Paunov, [a] and Nicole Pamme *[a]

[a] Department of Chemistry and Biochemistry, University of Hull, Cottingham Road, Hull, HU6 7RX, UK.
[§] Current address: Albaha University, Prince Mohammad Bin Saud, Al Bahah 65527, Saudi Arabia.
[‡] Current address: School of Earth and Environment, University of Leeds, Woodhouse Lane, Leeds, LS2 9JT, UK.

1. Characterisation of polyelectrolyte assembly on manganese carbonate particles ($MnCO_3$)

Layer-by-layer assembly was performed on $MnCO_3$, crystals ranging in diameter from 3 to 5 µm (PlasmaChem, Germany). 50 mg of the dry particles were dispersed in 1 mL of purified water for washing. The particles were vortexed and then collected by centrifugation at 5000 rpm for 3 min. The supernatant was pipetted off before being replaced with 1 mL of fresh water. 500 µL of this particle suspension was added to 500 µL of the anionic polyelectrolyte PSS (2 mg mL^{-1}) in a 1.5 mL Eppendorf tube and incubated for 20 min under continuous rotation at 40 rpm on a tube rotator. The coated microparticles were centrifuged at 600 rpm for 2 min; the supernatant was removed and the particles were washed three times with deionised water to ensure the removal of free PEs. The negatively charged coated particles were then re-suspended in 500 µL of NaCl (0.5 M) before adding the positively charged second PE, PAH-FITC (2 mg mL^{-1}) (**figure S1.1**). The same protocol was repeated to deposit ten layers of alternatingly charged PEs (PSS/PAH-FITC) on the magnetic particles. EDTA solution (0.3 M) was used to dissolve the particle cores.

As shown in **figure S1.2(a)**, the zeta potential alternated as oppositely charged PE layers were deposited on the particle cores. The fluorescence intensity was found to increase with the number of fluorescently-tagged PE layers (FITC-PAH) deposited (**figure S1.2(b)**). SEM images of the $MnCO_3$ cores before the LbL coating and of the collapsed hollow-shell PE capsules after the $MnCO_3$ core removal are shown in **figures S1.2(c-d)**. Microparticles coated with five bi-layers of FITC-PAH/PSS were also captured with fluorescence microscopy (**figure S1.2(e)**) and confocal microscopy (**figure S1.2(f)**) clearly showing the fluorescent polyelectrolyte embedded in the layers.

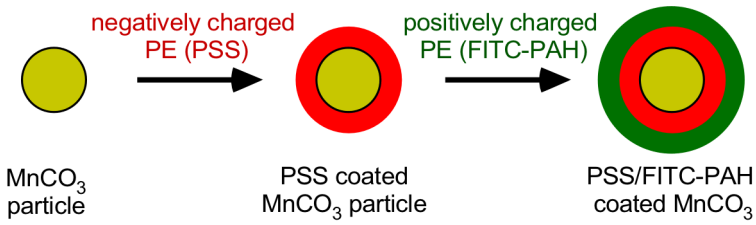

Figure S1.1 Schematic of the coating of $MnCO_3$ particles with alternating PE assembly of FITC-PAH and PSS. The $MnCO_3$ particles were exposed to a fluorescently-labelled, positively charged PE (FITC PAH) to deposit the first PE layer. The excess PE was removed by the cycles of centrifugation and washing steps before the second layer of negatively charged PEs (PSS) was added.

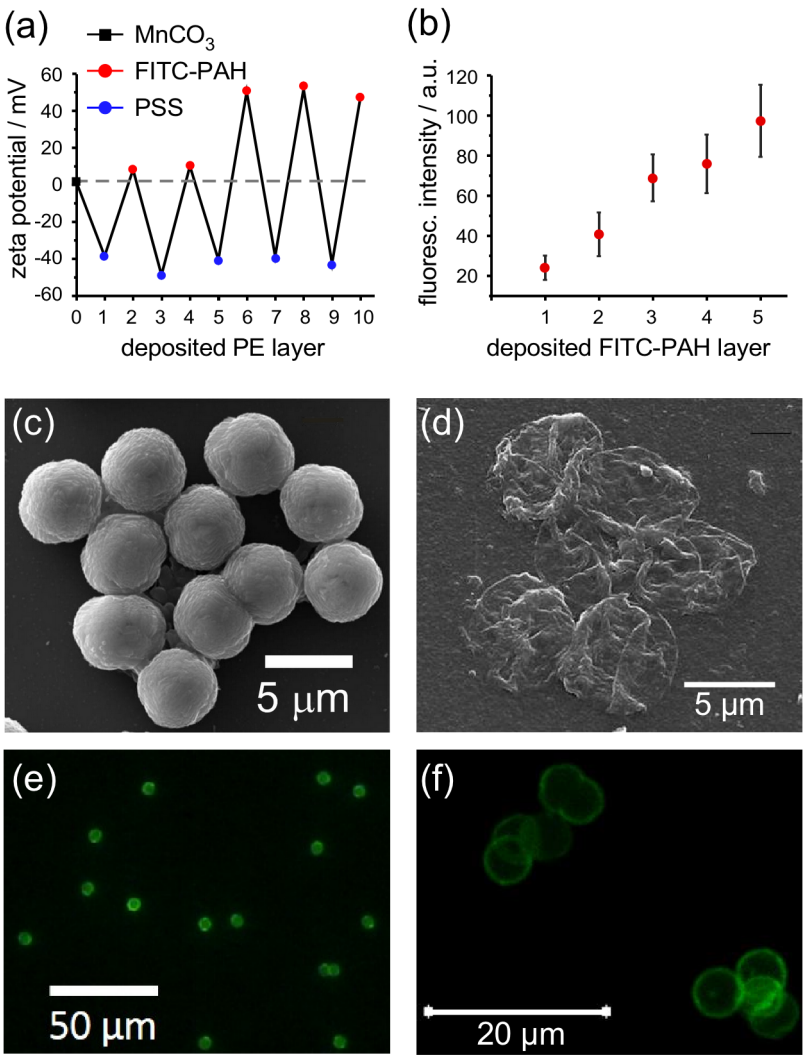

Figure S-1.2 PE layers deposited onto $MnCO_3$ crystals. (a) The zeta potential changes from positive to a negative demonstrating the alternating particle surface charge. (b) Fluorescence intensity plotted as a function of the fluorescent FITC-PAH layer number; the fluorescence increased indicating the successful PE film growth. (c) SEM image of the $MnCO_3$ cores before LbL coating and (d) collapsed hollow PE capsules after the $MnCO_3$ was removed with EDTA solution. (e) Fluorescence image of $MnCO_3$ particles and (f) CLSM of LbL capsules consisting of five bi-layers of FITCPAH/PSS.

2. Characterisation of polyelectrolyte assembly on calcium carbonate particles ($CaCO_3$)

Synthesis of calcium carbonate microparticles ($CaCO_3$)

Calcium carbonate microparticles ($CaCO_3$) were synthesised using procedures developed in the literature[1, 2]. Briefly, 1 mL of aqueous Na_2CO_3 solution (0.33 M) was poured rapidly into 1 mL of aqueous $CaCl_2$ solution (0.33 M) and mixed with a magnetic stirrer at 600 rpm for different periods of time (1 min, 5 min, 1 h, 2 h, 3 h) to study the effect of mixing time on particle morphology. The agitation was stopped and the particles were left for 10 min before washing three times with water. For this, the particle suspension was pipetted in an Eppendorf tube and vortexed for 15 s. The particles were collected via centrifuge at 5,000 rpm for 3 min, and finally the supernatant was removed and replaced with purified water. The $CaCO_3$ particles were re-suspended in 0.5 ml of 0.5M NaCl prior to the PE assembly (section 2.2). For SEM imaging (**figure S2.1**) the particles were thoroughly washed with purified water to remove the NaCl. The formation of uniform, nearly spherical $CaCO_3$ microparticles with narrow size distribution (4 ± 1 µm) was observed at a short mixing time (30 s) of Na_2CO_3 and $CaCl_2$; this condition was chosen for PE assembly.

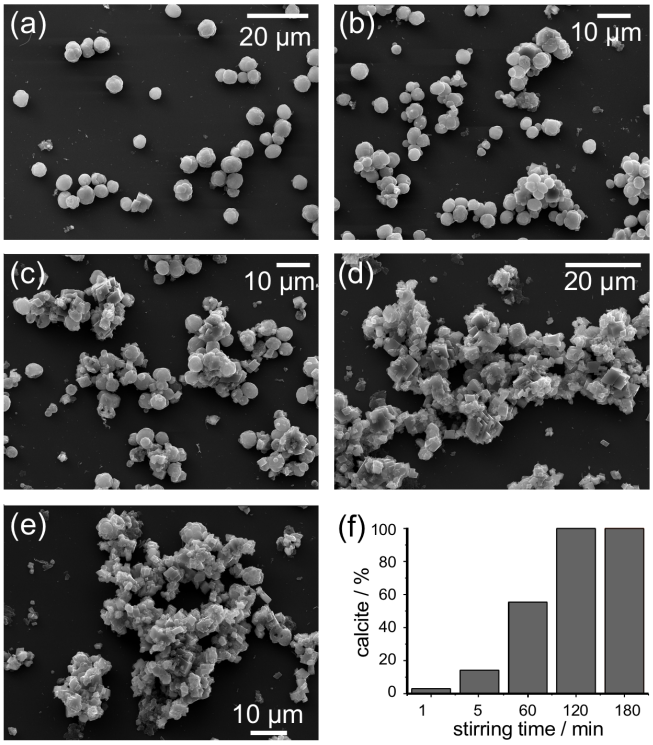

Figure S-2.1 SEM images of $CaCO_3$ microparticles obtained after different stirring periods during the synthesis process. (a) Spherical particles (vaterite) crystals obtained after mixing for 1 and (b) 5 min; (c) a mixture of spherical particles (vaterite) and rhombohedral microcrystals (calcite) obtained after stirring for 1 h; (d) rhombohedral microcrystals (calcite) obtained when stirring for 2 h and (e) 3 h. (f) Calcite microcrystal amount (%) as a function of stirring time.

PSS/PAH assembly on calcium carbonate particles ($CaCO_3$)

The process of LbL assembly of PE layers on the calcium carbonate particles is laid out in **figure S2.2**. 300 µL of $CaCO_3$ particle stock suspension were incubated in 1 mL of PAH polyelectrolyte (1 mg mL^{-1}) under continuous rotation for 15 min. The excess of PE was removed by three centrifugation and washing cycles with purified water (6,000 rpm, 3 min). Next, the microparticles were dispersed into 1 mL of PSS polyelectrolyte (1 mg mL^{-1}), followed by three rounds of washing. This LbL deposition was repeated until the desired number of PE layers were deposited on the microparticles. Zeta potential measurements and microscopy images confirm the layer deposition as shown in **figure S2.3**.

Hollow-shell PE microcapsules were obtained by dissolving the $CaCO_3$ core with EDTA. Different volumes of EDTA were added to the $CaCO_3$ particles and incubated for varying times to optimise the core dissolution. In the first experiment, 1 mL of fresh EDTA (0.3 M) was added to the coated $CaCO_3$ particles and vortexed for 2 h followed by centrifugation (1,200 rpm for 10 min) and re-dispersion in 1 mL of fresh EDTA. This step was repeated three times to ensure all particles had dissolved before the final rinse with purified water. In an alternative experiment, 10 mL of EDTA (0.3 M) were added to the particles and incubated for 20 h before the supernatant was removed and replaced with water. **Figure S2.4** shows examples of LbL-coated $CaCO_3$ microparticles following attempted EDTA core dissolution.

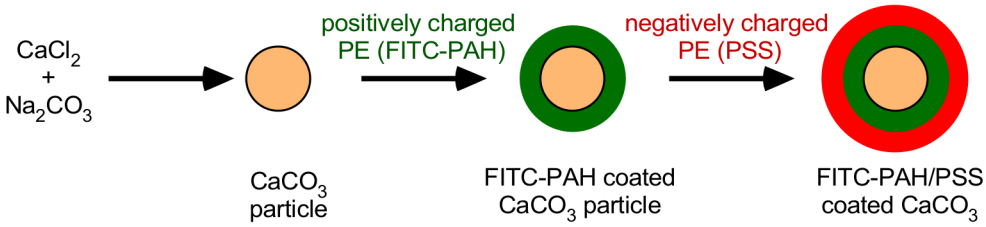

Figure S2.2 Schematics of the preparation and coating of the $CaCO_3$ particles with alternating layers of polyelectrolytes, namely positively charged FITC-PAH and negatively charged PSS.

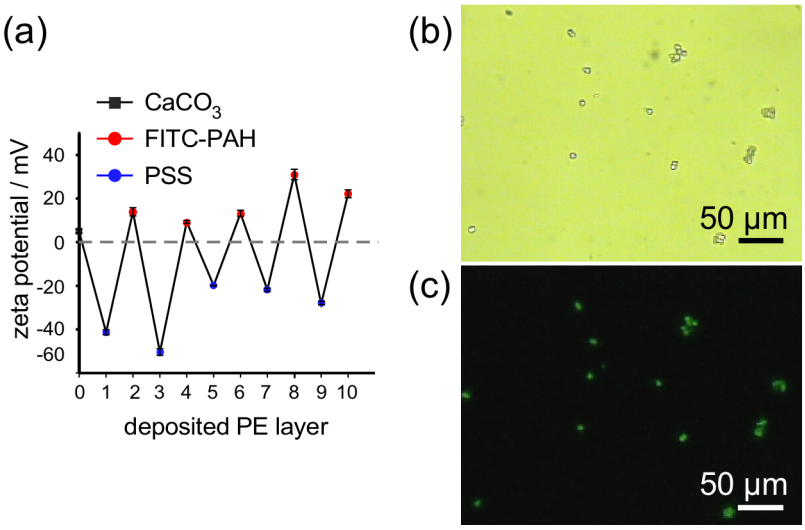

Figure S-2.3 LbL deposition of PE $(PSS/FITC\text{-}PAH)_5$ on $CaCO_3$ microparticles. (a) The particles zeta potential alternates as a function of the number PE layers deposited (n=3). (b) Bright field image and (c) fluorescence microscope image of $CaCO_3$ microparticles coated with 10 layers of FITC-PAH/PSS polyelectrolyte.

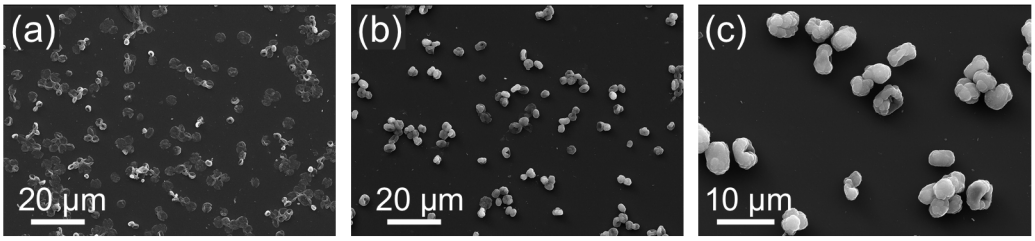

Figure S-2.4 SEM images of LbL formed PE microcapsules with particles core dissolved by EDTA solution. (a) Two-bilayered PE microcapsules forming a thinner shell. (b) Six-bilayer PE microcapsules with a thicker shell. (c) Ten-bilayer PE $CaCO_3$ particles with the majority of $CaCO_3$ cores not dissolved.

3. Streptavidin encapsulation efficiency in polyelectrolyte microcapsules templated on $MnCO_3$ or $CaCO_3$

Streptavidin incorporation into capsules made from $MnCO_3$ microparticles

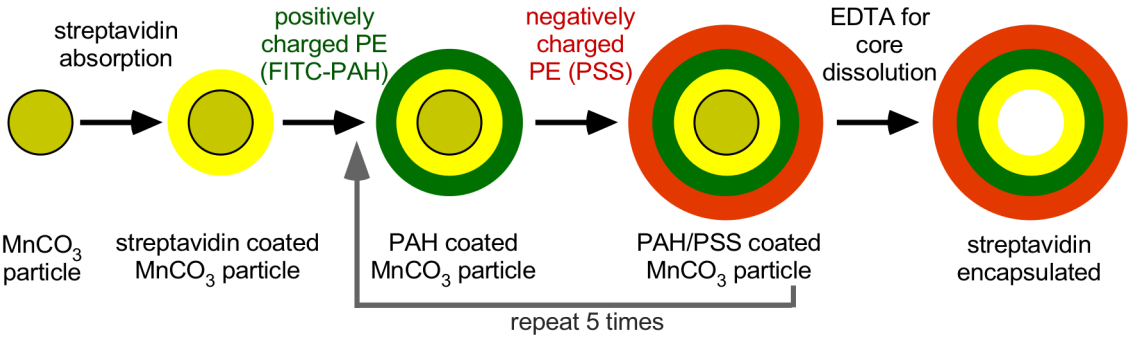

Figure S-3.1 Streptavidin was loaded directly onto the $MnCO_3$ microparticles, followed by deposition of alternating layers of polyelectrolytes, namely the cationic PAH and the anionic PSS. Five bilayers were deposited.

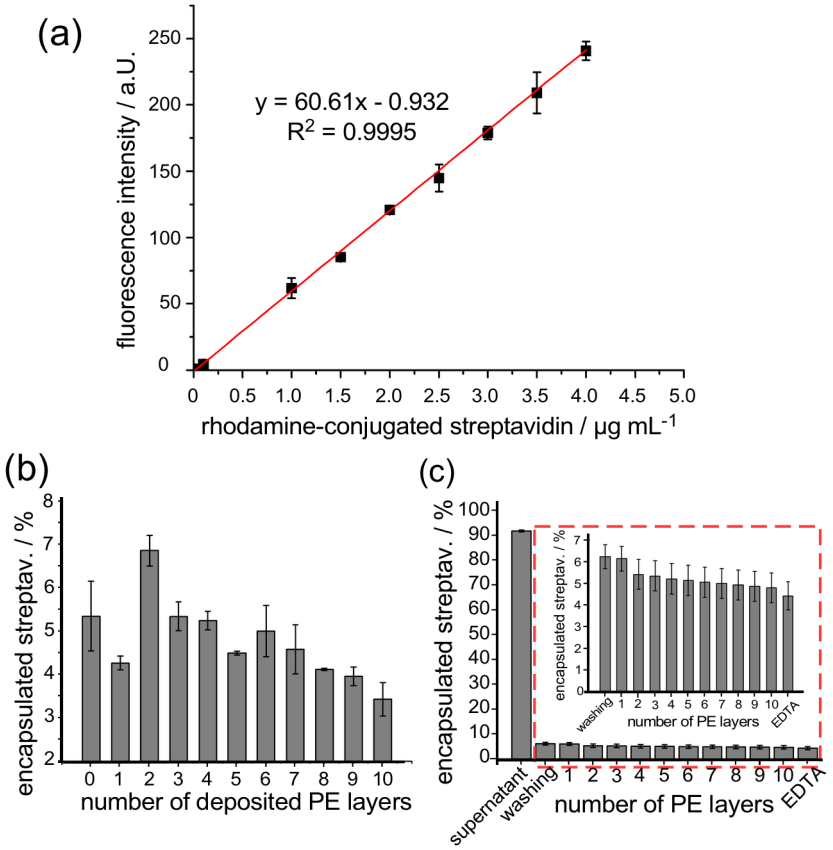

Figure S-3.2 (a) Calibration curve of Rhodamine Red™-X conjugated streptavidin. (b) The encapsulation efficiency (in %) of Rhodamine Red™-X conjugated streptavidin measured directly from the particle suspension. (c) Loss of streptavidin during the deposition of PE layers and core dissolution with EDTA solution. The magnified cross section shows the encapsulation efficiency (in %) of fluorescent streptavidin measured through streptavidin released into PE, washing and EDTA solutions.

Streptavidin incorporation into capsules made from $CaCO_3$ microspheres

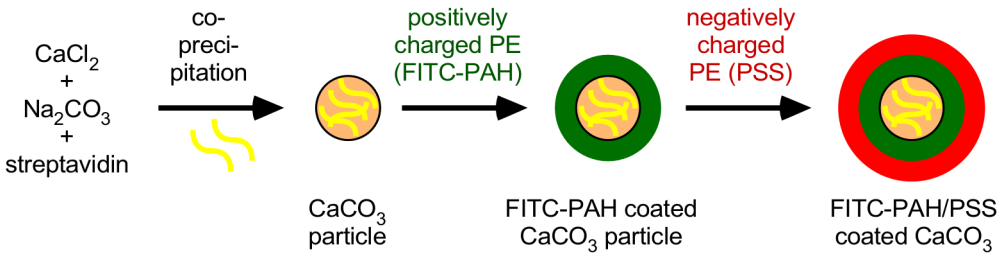

Figure S-3.3 Schematic of the method to encapsulate streptavidin inside $CaCO_3$ particles via the co-precipitation, followed by LbL assembly of PAH/PSS polyelectrolytes. During core formation, streptavidin is co-precipitated inside the $CaCO_3$ microparticles. PAH, a polycation PE, is deposited as the first layer. Excess PE is removed via washing before the second PE layer, PSS (a polyanion PE), is deposited. The core is then dissolved by EDTA to leave hollow capsules loaded with streptavidin.

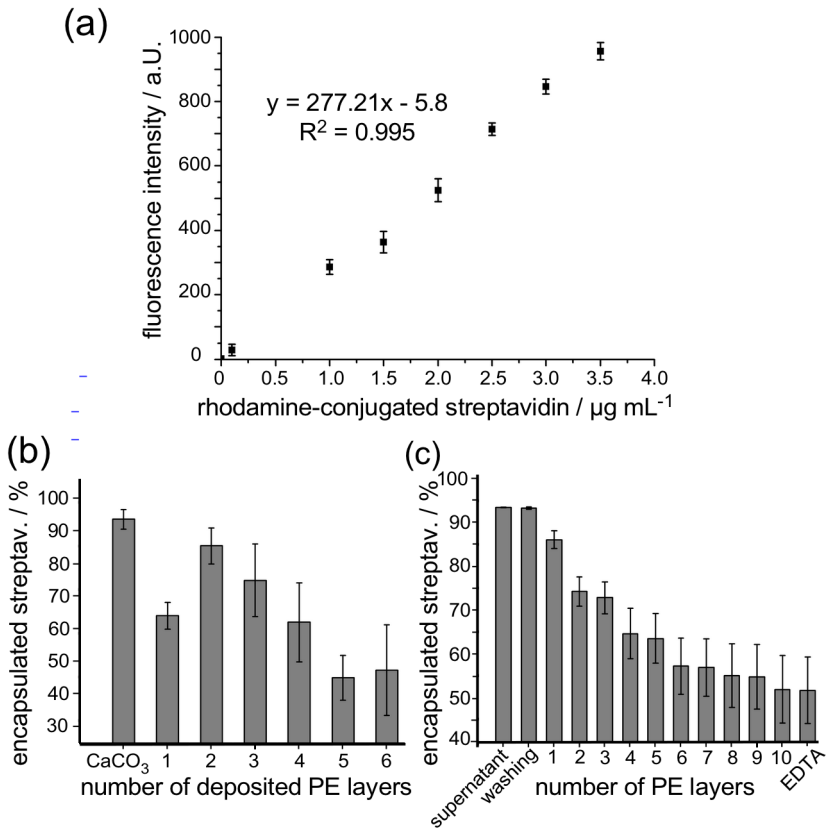

Figure S-3.4 (a) Calibration curve for rhodamine-conjugated streptavidin. Encapsulation efficiency (in %) of fluorescent streptavidin was measured (b) directly from the particle suspension, or (c) by the amount of streptavidin released into PE, washing and EDTA solutions during the LbL process.

4. Streptavidin-biotin assays carried out in polyelectrolyte microcapsules

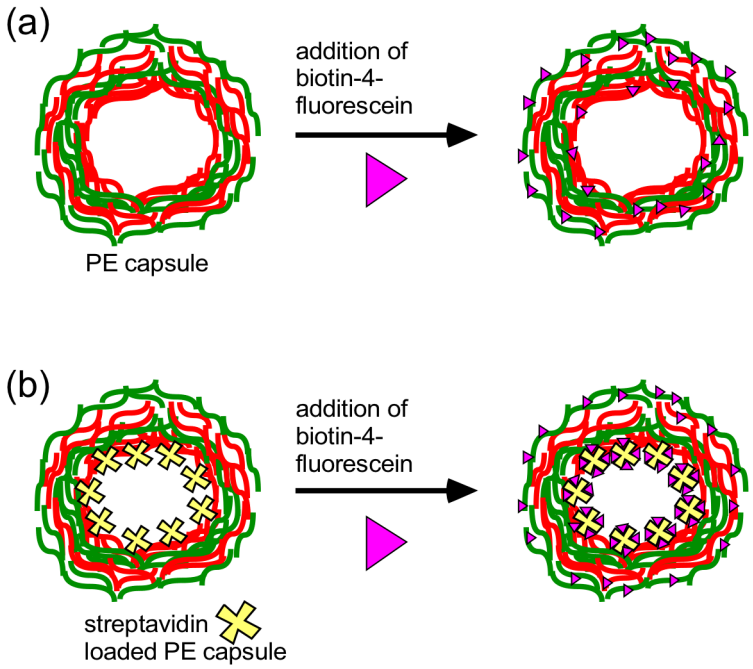

Figure S-4.1 Concept of streptavidin-biotin assay in LbL capsules templated from $MnCO_3$ and $CaCO_3$ microparticles. (a) Biotin-4-fluorescein solution was added to capsules not containing streptavidin as a control and (b) to PE capsules filled with streptavidin.

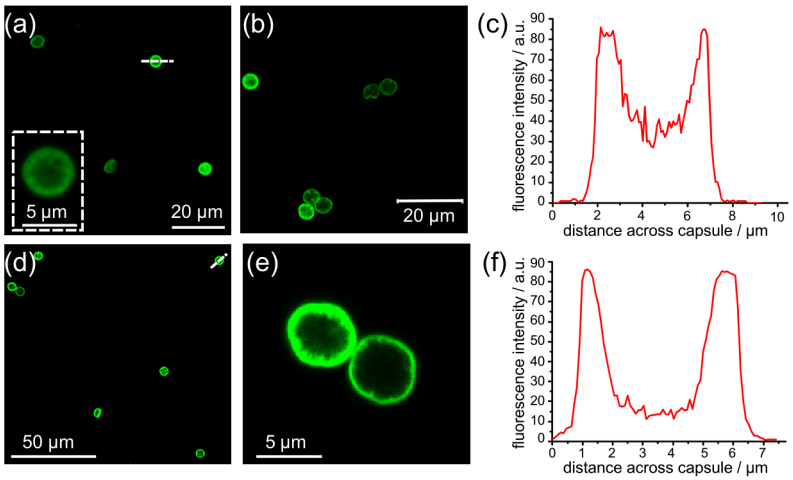

Figure S-4.2 Streptavidin-biotin assay performed in microcapsules templated on MnCO3 particles. (a, b) Fluorescence CLSM images of streptavidin-free microcapsules. (c) Fluorescence intensity profile for line plotted across streptavidin-free microcapsules. (d) Low magnification fluorescence CLSM image of streptavidin-loaded microcapsules. (e) High magnification fluorescence CLSM image of streptavidin-loaded microcapsules. (f) Fluorescence intensity profile across streptavidin-loaded microcapsule.

References

1. G. B. Sukhorukov, D. V. Volodkin, A. M. Gunther, A. I. Petrov, D. B. Shenoy and H. Mohwald, *Journal of Materials Chemistry*, 2004, **14**, 2073-2081.
2. D. V. Volodkin, A. I. Petrov, M. Prevot and G. B. Sukhorukov, *Langmuir*, 2004, **20**, 3398-3406.